Mem. S.A.It. Suppl. Vol. 1, 192

Memorie della
Supplementi

Dynamics of Oscillating Relativistic Tori

O. Zanotti[1] and L. Rezzolla[1,2]

[1] SISSA, International School for Advanced Studies, Via Beirut, 2-4 34014 Trieste, Italy

[2] INFN, Sezione di Trieste, Via Beirut, 2-4 34014 Trieste, Italy

Abstract. We present results of two-dimensional general relativistic hydrodynamical simulations of constant specific angular momentum tori orbiting a Schwarzschild black hole. Upon the introduction of axisymmetric perturbations, these objects either become unstable to the runaway instability or respond with regular oscillations. Among other things, these oscillations become responsible for the emission of intense gravitational radiation, with strain amplitudes large enough to be detected by the planned interferometric detectors.

Key words. accretion discs – general relativity – hydrodynamics – oscillations – gravitational waves

1. Introduction

Stationary non-Keplerian perfect fluid configurations around a black hole can be built in which the isobaric surfaces possess a sharp cusp on the equatorial plane (Abramowicz et al. 1978; Kozlowski et al. 1978). The cusp plays the role of a Lagrangian point and provides a simple mechanism for obtaining accretion even in the absence of a shear viscosity in the fluid. The dynamical response of these relativistic tori to perturbations has important astrophysical implications and will be discussed here in connection with the following three issues.

Firstly, the issue of stability with respect to the accretion of matter through the cusp. Any amount of material accreted onto the black hole, in fact, will affect the background spacetime and the location of the cusp itself. In particular, if the cusp moves to *larger* radial positions faster than the inner edge of the torus (which has shrunk as a result of the loss of mass), additional material will accrete onto the black hole. The new configuration will be not of equilibrium and produce the so called "runaway" instability (Abramowicz et al. 1983). The occurrence of this instability could have important implications on current models of γ-ray bursts (Daigne & Mochkovitch 1997; Meszaros 2002).

Secondly, the issue of the oscillation properties of relativistic tori. Having an internal structure governed by the balance of gravitational forces, pressure gradients and centrifugal forces, these relativistic tori respond to perturbations by oscillating at characteristic frequencies which can be computed to high precision. The possibility of calculating numerically the nonlinear hydrodynamical evolution of the torus provides, in fact, an excellent tool for studying discoseismology in two dimensions and General Relativity. Note also the during each of these oscillations a significant amount of matter falls into the black hole and it is reasonable to expect that before this matter reaches the event horizon it will loose part of its potential binding energy by emitting electromagnetic radiation. For this reason, it is possible that the quasi-periodic accretion measured during our simulations could also be observed in the form of a electromagnetic radiation in X-ray binaries (van der Klis 2000).

Thirdly, and maybe most importantly, the issue of the emission of gravitational waves. Because of their toroidal topology, in fact, the relativistic tori considered here have intrinsically large mass quadrupoles and if the latter are induced to change rapidly as a consequence of perturbations, large amounts of gravitational waves could be emitted and possibly detected.

A detailed description of how stationary configurations can be determined and a classification of the possible models is available in the literature (Abramowicz et al. 1978; Font & Daigne 2002a). The results presented here have been obtained by considering the response to perturbations of relativistic tori with finite extent and constant angular momentum (per unit energy).

2. Numerical Setup

As shown by Martí *et al.* (1991), the general relativistic Euler equations can be recast as a hyperbolic system of conservation laws, which take the form (Banyuls et al. 1997)

$$\frac{\partial \mathbf{U}}{\partial t} + \frac{\partial [\alpha \mathbf{F}^r]}{\partial r} + \frac{\partial [\alpha \mathbf{F}^\theta]}{\partial \theta} = \mathbf{S} \ , \qquad (1)$$

where $\alpha \equiv \sqrt{-g_{00}}$ is the lapse function of the Schwarzschild metric. $\mathbf{U} = (D, S_r, S_\theta, S_\phi)$ is the state-vector of the variables to evolve in time, i.e. of the relativistic rest mass density, of the momenta in the various coordinate directions and of the total energy density, as measured by an Eulerian observer in the Schwarzschild metric. The other vectors $\mathbf{F}^i$ and $\mathbf{S}$ appearing in (1) represent the fluxes and sources of the evolved quantities, respectively, with the latter being due entirely to the curvature of spacetime. Explicit expressions of all these terms can be found in Font & Daigne (2002a).

The conservative nature of the system (1) is the key ingredient for building numerical methods, also called Godunov type methods (see, e.g. Font (2000) and references therein), which guarantee high order of accuracy, sharp resolution of discontinuities and absence of spurious oscillations everywhere in the solution. In particular, second order accuracy both in time and in space is guaranteed after adopting Marquina's approximate Riemann solver for the calculation of the inter-cell numerical fluxes and a second order Runge-Kutta scheme for the time update (see Ibañez & Martí, 1999).

The computational grid, consisting of $(N_r \times N_\theta) = (250 \times 84)$ zones in the radial and angular directions covers a computational domain extending from $r_{\rm min} = 2.1\ M$ and to $r_{\rm max} = 30\ M$ and from 0 to π.

3. Evolution of the spacetime

To assess the occurrence of the runaway instability, it is essential that the changes in the spacetime are properly taken into account. In principle, this would require the solution of the Einstein equations as well as those of relativistic hydrodynamics. Apart from the intrinsic difficulty of this problem [see Shibata & Uryū (2000); Font et al. (2002) for recent developments] the need of high spatial resolution and the limited computing resources are still major obstacles to the goal.

To circumvent this, we have followed a more pragmatic approach, already suggested by Font & Daigne (2002a) and in which the metric terms are updated from a given time-level to the following one simply on the basis of the amount of matter which has accreted onto the black hole, i.e.

$$g_{\mu\nu}(r, M^n) \longrightarrow \tilde{g}_{\mu\nu}(r, M^{n+1}) \ , \qquad (2)$$

where $M^{n+1} = M^n + \Delta t \ \dot{m}^n(r_{\rm min})$ and $\dot{m}^n(r_{\rm min})$ is the rest-mass accretion rate measured at the event horizon. Within this approach then, the evolution of the black hole spacetime is made in terms of a sequence of stationary Schwarzschild solutions and we refer to this as to a *"dynamical"* spacetime. Of course, this represents an approximation to the correct evolution and, in particular, it prevents us from quantifying the response of the black hole to the accreted mass and the corresponding emission of gravitational radiation. Nevertheless, this is a rather good approximation, especially when the the mass of the torus is small as compared to that of the black hole and the rest-mass accretion rates are small.

4. Initial Data: perturbing the stationary solution

In our calculations, an initial stationary solution constructed following the procedure suggested by Abramowicz et al. (1978), is perturbed by introducing a small radial velocity field, which is chosen as a parametrization of the spherical accretion solution in a Schwarzschild spacetime, i.e. the Michel solution (Michel 1972). In other words, we introduce a nonzero radial velocity v_r such that

$$v_r = \eta (v_r)_{\rm Michel} \ , \qquad (3)$$

where η is the parametric strength of the perturbation and $(v_r)_{\rm Michel}$ is the radial velocity in the Michel solution. It is worth stressing that our initial conditions are rather realistic as they tend to reproduce the physical conditions in which these tori are presumed to be formed. We recall, in fact, that tori of the type considered here are expected to form in a number of different events such as the collapse of supermassive neutron stars (Vietri & Stella 1998), or the iron-core collapse of a massive stars (MacFayden & Woosley 1999). Other scenarios for the genesis of these objects involve the coalescence of a binary system, either consisting of two neutron stars or consisting of a black hole and of a neutron star which is then disrupted by the intense tidal field (Lee &Kluzniak 1999a; Lee & Kluzniak 1999b; Lee 2000). In all of these catastrophic events, the newly formed torus will be initially highly perturbed and is expected to maintain also a radial velocity in addition to the orbital one. In recent Newtonian simulations performed by Ruffert & Janka (1999) the torus resulting from the dynamical merging of two neutron stars was observed to oscillate and accrete onto the newly formed black hole with an averaged inflow velocity in the central region of the order of $\sim 3 \times 10^{-3}c$. The values of the parameter η have therefore been chosen so as to be compatible with the estimates provided by Ruffert & Janka (1999) and are in the range $[0.001, 0.06]$.

5. Numerical results

5.1. Runaway instability

Through a number of hydrodynamical simulations, Font & Daigne (2002a) were able to show that, for *constant* specific angular momentum tori slightly overflowing their Roche lobes, the runaway instability does take place and for a wide range of ratios between the mass of the torus and that of the black hole. Our simulations, performed with a dynamical spacetime and using the initial conditions discussed in Section 4, have confirmed the results obtained by Font & Daigne (2002a). In addition to this, however, our results also indicate that the runaway instability does occur also with this choice of initial data and that the growth-rate is shorter for larger initial velocity perturbations (i.e. for larger values of η). This is an important point underlining that Roche lobe overflowing is not a necessary condition for the development of the instability, at least in constant

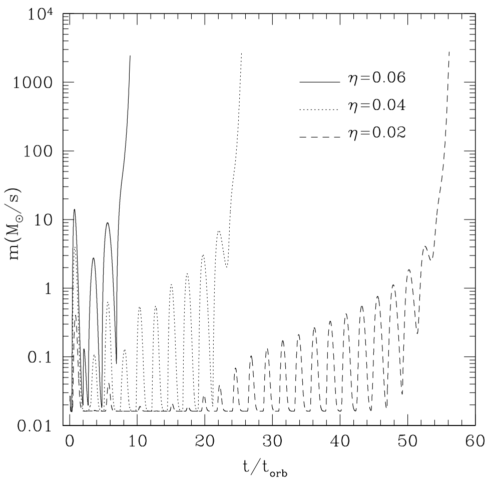

Fig. 1. Evolution of the rest-mass accretion rate for a model having a torus-to-hole mass ratio equal to unity. Three different values of η have been chosen and the spacetime is allowed to vary. The time is expressed in terms of the orbital period $t_{\rm orb} = 1.87$ ms.

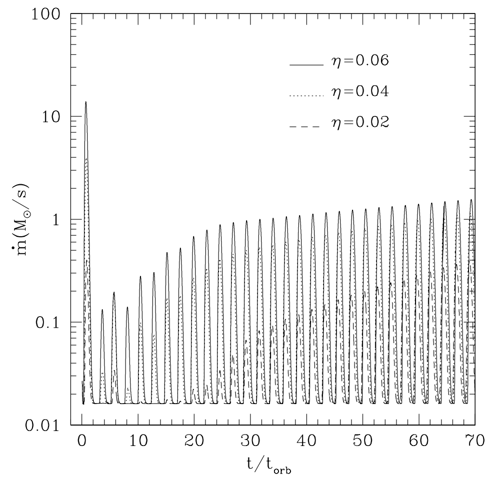

Fig. 2. Rest-mass accretion rate in a fixed spacetime evolution.

specific angular momentum tori whose self-gravity is not considered. Figure 1 shows the evolution of the rest-mass accretion rate in a typical model for three different values of initial velocity perturbation, η. The time is expressed in terms of the orbital period $t_{\rm orb} \equiv 2\pi/\Omega_{\rm centre}$ of the centre of the torus, which is $t_{\rm orb} = 1.87$ ms for this specific model. As it is apparent from Figure 1, the accretion rate grows exponentially after a timescale which is shorter for larger values of the initial velocity perturbations. During the full development of the instability, the calculations become very difficult and Courant factors as small as 0.01 must be taken in order to avoid the crashing of the code, (see Zanotti et al. (2002) for further details).

Another important feature to note in Figure 1 is that the secular growth in the rest-mass accretion rate is *also* accompanied by an oscillatory behaviour with increasing amplitude. This suggests that the torus is experiencing a series oscillations (basically compressions and expansions) and that during each of these oscillations a considerable amount of matter falls towards the black hole.

5.2. Quasi-periodic behaviour

When concentrating on the quasi-periodic response of the torus to perturbations, the occurrence of the runaway instability represents a complication to avoid. Since the actual occurrence of the instability is still under debate and can be suppressed if the specific angular momentum distribution is increasing sufficiently fast in radius (Font & Daigne 2002b), we have also investigated scenarios in which the runaway instability does not occur. To do this in practice, we simply have carried simulations in which the metric functions are not updated as detailed in equation (2) but are rather held constant in time. This is sufficient to suppress the occurrence of the runaway instability and we refer to these evolutions as with a *"fixed"* spacetime.

Figure 2 shows the evolution of the accretion rate during the first 30 orbital periods for a simulation in which the spacetime is held fixed. Similarly to the case of

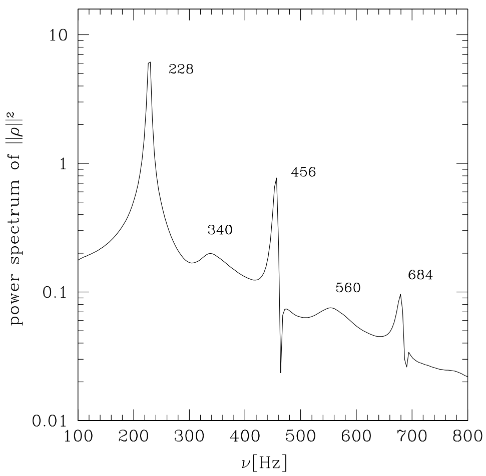

Fig. 3. Power spectrum of the mass accretion rate for the models shown in Figure 2.

the dynamical spacetime, the amplitude of the mass accretion rate manifests a dependence on the value of η, but never diverges. Therefore, the pulsating behaviour can now be studied on its own, regardless of the development of the instability. Each period of oscillation in Figure 2 is the result of numerical calculations requiring several tens of thousands timesteps, thus confirming the excellent performances of HRSC methods in reproducing subtle hydrodynamical effects with very high precision. The mass accretion rate is not the only quantity showing a periodic behaviour and indeed all of the fluid variables can be shown to oscillate periodically.

In Figure 3 we plot the power spectrum of the L_2 norm of the rest-mass density (i.e. an integral quantity over the numerical grid) for the models reported in Figure 2. The Fourier transform has been calculated with data obtained with an $\eta = 0.06$ perturbation and computed over a time interval going up to $t/t_{\rm orb} \simeq 100$. As it is evident from Figure 3, the power spectrum consists of a fundamental frequency (at 228 Hz for the model considered in Figure 3) and a series of overtones (at 340, 456 Hz, etc.) in a ratio which can be determined to be $2:3:4\ldots$ and to an accuracy of a few percent. This suggests that the quasi-periodic response observed is the consequence of some fundamental mode of oscillation of the torus.

After carrying a linear perturbative analysis of vertically integrated relativistic tori (Rezzolla et al. 2002), we have concluded that the modes observed in the numerical simulations correspond to global p-modes (or pressure modes) of oscillation of the torus. Furthermore, it is possible to show that p-modes in a general non-Keplerian disc represent the vibrational modes of relativistic tori having pressure gradients as the restoring forces and appear with the characteristic ratio $2:3:4:\ldots$ that the simulations have revealed (Rezzolla et al. 2002).

5.3. Gravitational wave emission

Although our treatment of the spacetime evolution in principle prevents us from calculating in General Relativity the gravitational radiation emitted during the accretion and the oscillations of the torus, the gravitational wave emission can still be estimated within the Newtonian quadrupole approximation. The interest in doing so comes from the fact that during the oscillations the tori undergo large and rapid variations of their mass quadrupole moment and this could make them potentially important sources of gravitational waves.

Within the Newtonian approximation then, the gravitational waveform $h^{TT}(t)$ observed at a distance R from the source is given by the quadrupole wave amplitude $A_{20}^{\rm E2}$ (see Zwerger & Müller 1997)

$$h^{TT}(t) = \left(\frac{1}{8}\sqrt{\frac{15}{\pi}}\right)\frac{A_{20}^{\rm E2}(t-R)}{R}\ , \qquad (4)$$

where the wave amplitude $A_{20}^{\rm E2}$ in equation (4) is simply given by the second time derivative of the mass quadrupole moment. Within this approximation, we have calculated the gravitational waves emitted during the periodic oscillations described

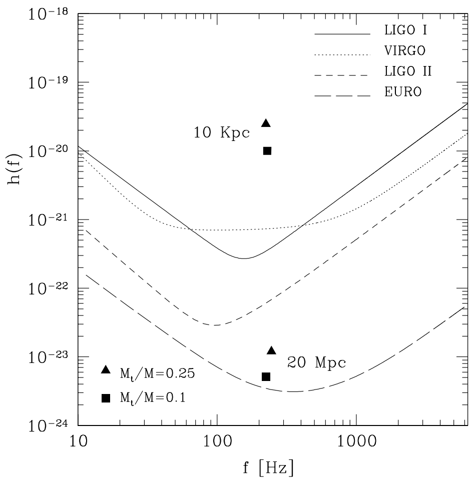

Fig. 4. Characteristic wave amplitudes for a perturbed relativistic torus with $\eta = 0.04$. These amplitudes have been computed using the strain noise estimated for LIGO I for a source located at a distance of 10 Kpc and for LIGO II for a source at a distance of 20 Mpc. The sensitivity curves of VIRGO and EURO have also been reported. Different points refer to different mass ratios, with triangles indicating $M_t/M = 0.25$ and squares $M_t/M = 0.1$.

above. More precisely, using Eq. (4) we have derived a phenomenological expression for the gravitational waveform that could be expected as a result of the oscillations induced in the torus. In particular, for a source located in the Galaxy, the transverse traceless gravitational wave amplitude can be expressed as

$$h^{TT} \simeq 2.2 \times 10^{-21} \left(\frac{\eta}{0.04}\right) \left(\frac{M_{\rm t}}{0.1\ M_{2.5}}\right) \times \left(\frac{10\ {\rm Kpc}}{R}\right) , \quad (5)$$

where $M_{2.5} \equiv M/(2.5\ M_{\odot})$. Expression (5) shows that, already in the linear regime for the parameter η, a non-negligible gravitational wave amplitude can be produced by an oscillating relativistic torus orbiting around a black hole. This amplitude is indeed comparable with the average gravitational wave amplitude computed in the case of core collapse in a supernova explosion (Dimmelmeier et al. 2002) and can become stronger for larger perturbations or masses in the torus.

In order to assess the detectability of relativistic tori as sources of gravitational radiation we have computed the *characteristic* gravitational wave frequency and amplitude (Thorne 1987) for the interferometric detectors that will soon be operative.

Figure 4 shows the characteristic wave amplitude for sources located at a distance of $R = 10$ Kpc and $R = 20$ Mpc, as computed for two different values of the torus-to-hole mass ratio.

Interestingly, with small initial perturbations ($\eta = 0.04$) and mass ratios ($M_{\rm t}/M = 0.1$), the computed characteristic amplitudes can be above the sensitivity curves of LIGO I for sources within 10 Kpc and above the sensitivity curve of EURO for sources within 20 Mpc. Both results allow us to consider oscillating relativistic tori as promising new sources of gravitational waves.

6. Conclusions

We have studied in detail the dynamics of oscillating relativistic tori by performing two-dimensional numerical simulations using HRSC methods. We have first confirmed that, at least for constant specific angular momentum tori whose self-gravity is neglected, the initial Roche lobe overflow is not a necessary condition for the development of the runaway instability, which then represents a natural feature of the dynamics of these objects in an evolving spacetime.

We have also shown that upon the introduction of suitably parametrized perturbations in the radial velocity field, the tori manifest a regular oscillatory behaviour resulting both in a quasi-periodic variation of the mass accretion rate as well as of the rest-mass distribution. This response has been interpreted in terms of the excitation of p-modes having pressure gradients as restoring forces and appearing with overtones in the ratio $2 : 3 : 4 : \ldots$.

Finally, as a consequence of the excitation of oscillations, the mass quadrupoles are induced to change rapidly and intense gravitational radiation is thus produced. We have made estimates within the Newtonian quadrupole approximation and shown that strong gravitational waves can be produced during the short lifetime of these tori. In particular, the gravitational radiation emitted by these sources is comparable or larger than the one that is expected during the gravitational collapse of a stellar iron core.

Acknowledgements. It is a pleasure to thank J. A. Font and S'i. Yoshida for collaborating with us on these projects. Special thanks also go to Roberto Capuzzo Dolcetta for promoting the first of this series of conferences. Financial support for this research has been provided by the MIUR and by the EU Network Programme (Research Training Network Contract HPRN-CT-2000-00137). The numerical computations were performed on the Beowulf Cluster for numerical relativity *"Albert100"*, at the University of Parma.

References

Abramowicz M. A. Jaroszyński M. & Sikora M., 1978, A&A, 63, 221.

Abramowicz M. A., Calvani M., Nobili L., 1983, Nature, 302, 597

Banyuls F., Font J. A., Ibáñez J. M., Martí J. M., Miralles J. A., 1997, ApJ, 476, 221

Daigne F., Mochkovitch R., 1997, MNRAS, 285, L15

Dimmelmeier H., Font J. A., Müller E., 2002, A&A, 393, 523

Font J. A., 2000, Living Reviews in Relativity, 3, 2

Font J. A., Goodale T., Iyer S., Miller M., Rezzolla L., Seidel E., Stergioulas N., Suen W., Tobias M., 2002, Phys. Rev. D 65, 084024

Font J. A., Daigne F., 2002a, MNRAS, 334, 383

Font J. A., Daigne F., 2002b, ApJL, *in press*

Ibañez J. M., Martí J. M. 1999, J. Comp. Appl. Math., 109, 173

Kozlowski M., Jaroszynski M., Abramowicz M. A., 1978, A&A, 63, 209

Lee W. H., Kluzniak W., 1999a, MNRAS, 308, 780

Lee W. H., Kluzniak W., 1999b, ApJ, 526, 178

Lee W. H., MNRAS, 318, 606

MacFayden A. I., Woosley S. E., 1999, ApJ, 524, 262

Martí, J.M., Ibañez, J. M., Miralles, J. A. 1991, Phys. Rev. D 43, 3794

Meszaros P., 2002, ARA&A, 40, 137

Michel F., 1972, Astrophys. Spa. Sci., 15, 153

Rezzolla L., Yoshida S'i., Zanotti O., 2002 *in preparation*

Ruffert M., Janka H.-T., 1999, A&A, 344, 573

Shibata M., Uryū K., 2000, Phys. Rev. D, 61, 4001

Thorne K. S. in *300 Years of Gravitation*, edited by S. W. Hawking ans W. Israel, Cambridge University Press, Cambridge, England, 1987

van der Klis M., 2000, ARA&A, 38, 71

Vietri M., Stella L. 1998, ApJ. 507, L45

Zanotti O., Rezzolla L., Font A. J., 2002, MNRAS, *submitted*

Zwerger T., Müller E., 1997, A&A, 320, 209